Electronic Supplementary Material (ESI) for ChemComm.

Supplementary Information

Monitoring the Evolution of Local Oxygen Environments during $LiCoO_2$ Charging via ex situ ^{17}O NMR

Fushan Geng, Ming Shen, Bei Hu, Yufeng Liu, Lecheng Zeng and Bingwen Hu*

*. Shanghai Key Laboratory of Magnetic Resonance, State Key Laboratory of Precision Spectroscopy, School of Physics and Materials Science, East China Normal University, Shanghai 200062, China

E-mail: bwhu@phy.ecnu.edu.cn

Experimental Procedures

Material synthesis.

Synthesis of ^{17}O labelled $LiCoO_2$. First, CoOOH was prepared as the precursor. In a typical synthesis, $Co(NO_3)_2{\cdot}6H_2O$ (Aladdin) and KOH (Aladdin) with a molar ratio of 1: 2.5 were dissolved in beakers respectively, and then they were mixed to form pink precipitates of $Co(OH)_2$. 30% H_2O_2 liquid was added into the suspension drop by drop under magnetic stirring until the color of the suspension turned into brown. The precipitates were collected by vacuum filtration, and were washed with deionized water and dried at 90°C overnight. XRD characterization confirmed that the final product was β-CoOOH.

For the Synthesis of ^{17}O labelled $LiCoO_2$, 0.0055 mol of Li_2O (Aladdin), 0.01 mol of β-CoOOH and 0.5 mL of $H_2{}^{17}O$ (35–40% ^{17}O, Cambridge Isotope) were ground thoroughly for 30 minutes in a 45-mL zirconia grinding bowl with two yttria-stabilized zirconia balls (8 mm diameter), using a SPEX 8000M Mixer/Mill. Next, the mixture was calcinated at 750°C with a heating rate of 5°C min^{-1} under argon flow for 4 h in a tube furnace. The product was collected and manually ground in an agate mortar before preserved in an argon-filled glove box. The yield was about 1.5 g enough for the battery test.

Besides the low cost and rapid fabrication, this labeling procedure leads to a homogeneous distribution of ^{17}O atoms in the material, which is in favour of the investigation of all oxygen sites.

Synthesis of ^{17}O labelled Li_2MnO_3 and Li_2RuO_3. The grinding process was the same as that in the synthesis of ^{17}O labelled $LiCoO_2$, except that 0.0108 mol of Li_2O and 0.01 mol of MnO_2 (Aladdin) were used for synthesizing Li_2MnO_3 and 0.0115 mol of Li_2O and 0.01 mol of RuO_2 (Aladdin) were used for Li_2RuO_3. The calcination temperature was 750°C and 850°C for Li_2MnO_3 and Li_2RuO_3 respectively. Other conditions and operations stayed the same.

XRD Characterizations.

The powder XRD pattern of the ^{17}O-labeled $LiCoO_2$ was recorded with a Bruker D8-Advance diffractometer using a Cu $K_{\alpha1}$ radiation (λ = 1.5406 Å). The spectrum was collected in the 2θ range of 10–90°, at a scan rate of 0.5° min^{-1} with a step size of 0.02°. Rietveld refinement was carried out with the FullProf Suite software. The powder XRD patterns of the ^{17}O-labeled Li_2MnO_3 and Li_2RuO_3 were recorded with a Rigaku Ultima IV diffractometer using a Cu $K_{\alpha1}$ radiation (λ = 1.5406 Å).

Electrochemical delithiation.

The working electrodes were prepared via mixing the active material, Super P conductive agent and polyvinylidene difluoride (PVDF) in a weight ratio of 85:7.5:7.5 with drops of N-Methyl-2-pyrrolidone (NMP). Then the slurry was pasted on an aluminum foil, dried at 100°C overnight in vacuum and pressed with a desktop roller presser.

CR2032 coin cells were assembled in an argon filled glovebox with O_2 and H_2O concentration less than 1 ppm, using the prepared working electrodes, metallic lithium disks, separators (Celgard 2300), and 1 M $LiPF_6$ dissolved in a mixture of ethylene carbonate (EC), dimethyl carbonate (DMC) and ethyl methyl carbonate (EMC) (1:1:1 V/V/V) with additive of fluoroethylene carbonate (FEC) as the electrolyte. Galvanostatic charge tests were carried out on a Land CT2001A autocycler at a current density of 10 mA g^{-1}.

Solid-state NMR experiments.

Rotor Filling. Coin cells were carefully disassembled without short circuiting. Then every removed electrode was immersed in 2 mL of DMC for about 5 h and dried naturally to remove the residual electrolyte. The cycled materials were carefully scraped from the aluminum foils and filled into 2.5 mm zirconia rotors. All the operations were conducted in the argon filled glovebox.

Experimental details. All NMR experiments were performed on a 14.1T Bruker Advance III spectrometer at room temperature.

For ^{7}Li NMR, a rotor-synchronized Hahn-echo sequence with a π/2 pulse width of 1.6 μs was adopted, and the spinning speeds were controlled at 24 kHz or 27.5 kHz depending on the position of sidebands. The number of transients ranged from 64 to 2048 (22000 for x = 0.07), and the recycle delays from 50 to 2 s, depending on the x in Li_xCoO_2. ^{7}Li chemical shifts were externally referenced to 1 M LiCl solution at 0 ppm.

For ^{59}Co NMR, a rotor-synchronized Hahn-echo sequence with a π/2 pulse width of 1.5 μs was adopted, and the experiments were run at a spinning speed of 24 kHz. The recycle delays were set to 1.0 s for all the experiments except for the pristine $LiCoO_2$ using 10 s and $Li_{0.85}CoO_2$ using 3.0 s, and the number of transients ranged from 400 to 4000, depending on the x in Li_xCoO_2. The ^{59}Co NMR spectra were calibrated according to the previous reports.[1, 2]

A single π/2 pulse with a width of 2.5 μs with spinning speeds of 24 kHz was used to obtain the best signal to noise in ^{17}O NMR experiments. The use of Hahn-echo sequence led to halved signal to noise due to considerable T_2 relaxation during echo time. The relaxation delays were 0.2 s for all the experiments except for the pristine $LiCoO_2$ using 10 s and $Li_{0.85}CoO_2$ using 1.0 s. The number of transients for the pristine $LiCoO_2$ was 50,000 and the others were 300,000. For the ^{17}O NMR experiments at x = 0.4 and x = 0.18, a rotor-synchronized spin-echo sequence was used to get the right phase with spinning speeds of 26 and 24 kHz respectively. The relaxation delays were 0.1 s, and the number of transients were added to 800,000. The ^{17}O NMR experiments in a wider spectral window were performed with a single 3π/10 pulse with a width of 1.5 μs, and the other parameters were kept the same. ^{17}O chemical shifts were externally referenced to water at 0 ppm.

It is noted that for single pulse acquisition there existed a serious baseline distortion due to phase evolution of signals spanning large frequency domain. Therefore, left shifting the FID points was used to adjust the baseline as well as to find the befitting phase. The opposite phase of ^{17}O signals from the zirconia rotor is thus inevitable for better presenting the main signal.

Normalization. All the ex situ NMR spectra were normalized with respect to the mole number (n_x) of Li_xCoO_2 in the rotors and number of transients. Normalized data = Experimental data / (n_x × Number of transients); $n_x = m_x \times x\% / M_x$, where m_x is the total mass of the electrode powder filled in the rotor, x% is the percentage of the active materials (Li_xCoO_2) in the powder, and M_x is the molar mass of Li_xCoO_2. The calculation of x% is indicated in the following; all calculated parameters are listed in Table S1:

$$x\% = \frac{85 - 85 \times \left(1 - \frac{m_x}{m_1}\right)}{100 - 85 \times \left(1 - \frac{m_x}{m_1}\right)}$$

^{17}O NMR spectral fitting. The experimental ^{17}O spectra were fitted by DMFIT program.[3] The QUASAR module and the Q MAS 1/2 module were used to fit the ^{17}O spectrum of the pristine

$LiCoO_2$ and $Li_{0.4}CoO_2$ respectively.

Table S1. Normalization parameters.

x	1.00	0.85	0.75	0.67	0.56	0.50	0.40	0.31	0.18	0.07
m_x / mg	16.81	17.14	16.90	16.06	17.48	17.81	16.89	16.36	17.28	18.47
M_x / g mol^{-1}	97.87	96.86	96.14	95.56	94.83	94.37	93.71	93.05	92.17	91.45
x%	85.00	84.87	84.77	84.69	84.59	84.53	84.44	84.34	84.22	84.11
n_x / mmol	0.1460	0.1502	0.1490	0.1423	0.1559	0.1595	0.1522	0.1483	0.1579	0.1699

Further Explanation on the Signal Loss of ^{59}Co and ^{17}O NMR

The observability of a NMR signal in paramagnetic environments can be estimated by the condition $|A/h| << 1/T_{1e}$, where A/h is the hyperfine coupling constant and T_{1e} is the electron spin-lattice relaxation time.[4] When the condition is satisfied, the NMR signal may be observable. A typical T_{1e} is on the order of 10^{-8}~10^{-9} s, so when A/h is greater than 10 MHz, the NMR signal is very likely no longer observable. The hyperfine coupling constant could be very large if the nuclear and electronic spins belong to the same atom, such as the situation of Co^{4+}. In addition, those atoms directly bonding to the paramagnetic center will also have a large hyperfine coupling constant. The ^{17}O NMR signal loss was also found in paramagnetic coordination compounds, [Cu([$^{17}O_2$]-DL-alanine)$_2$]·H_2O and K_2[Cu([$^{17}O_4$]oxalate)$_2$]·$2H_2O$, due to the coordination of oxygen atoms to Cu(II) center as an axial ligand.[5]

Li atoms are separated by two bonds from the paramagnetic Co^{4+}, and the bonding is more ionic. Therefore, the hyperfine interaction is relatively weak, which leads to a smaller A/h. We can observe a Knight-shifted signal due to the Fermi-contact interaction when the amount of Co^{4+} is increasing.

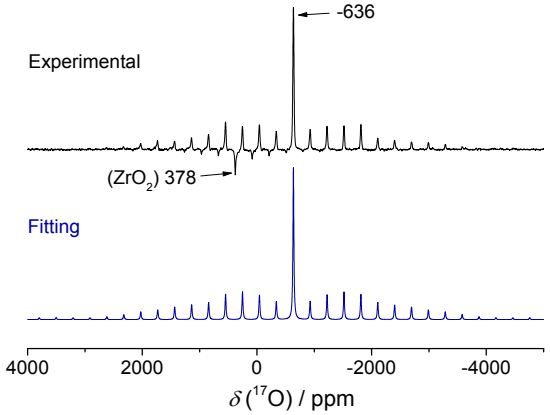

Figure S1. ^{17}O MAS NMR spectrum (top) and the spectral fitting (bottom) of ^{17}O-labeled $LiCoO_2$. The spectrum is recorded at 14.1 T and 24 kHz MAS. A single π/2-pulse with a pulse width of 2.5 μs was adopted in order to obtain the best signal to noise. The spectral fitting shows a single oxygen site with a quadrupolar coupling constant (C_Q) of 1.47 MHz and an asymmetry parameter (η) of 0.21.

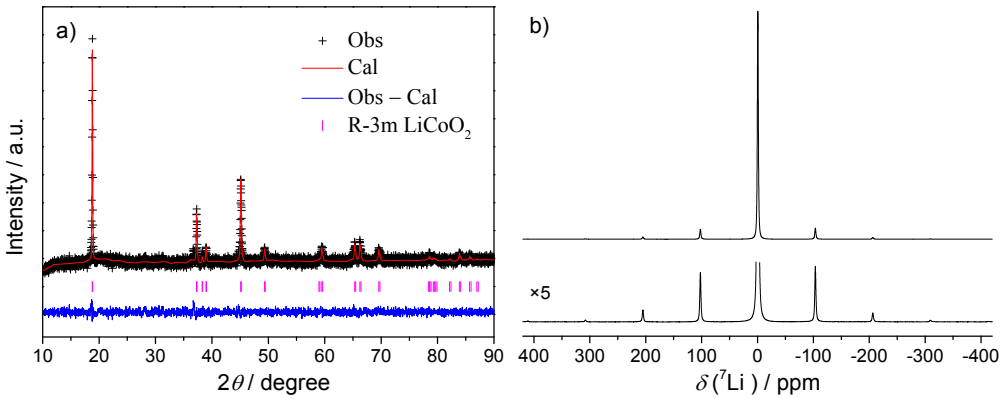

Figure S2. Rietveld refinement of the XRD pattern (a) and ^{7}Li NMR spectrum (b) of the ^{17}O-labeled $LiCoO_2$. Trace impurity of Co_3O_4 can be identified by the diffraction at 2θ = 36.7°. Nevertheless, it does not influence NMR results.

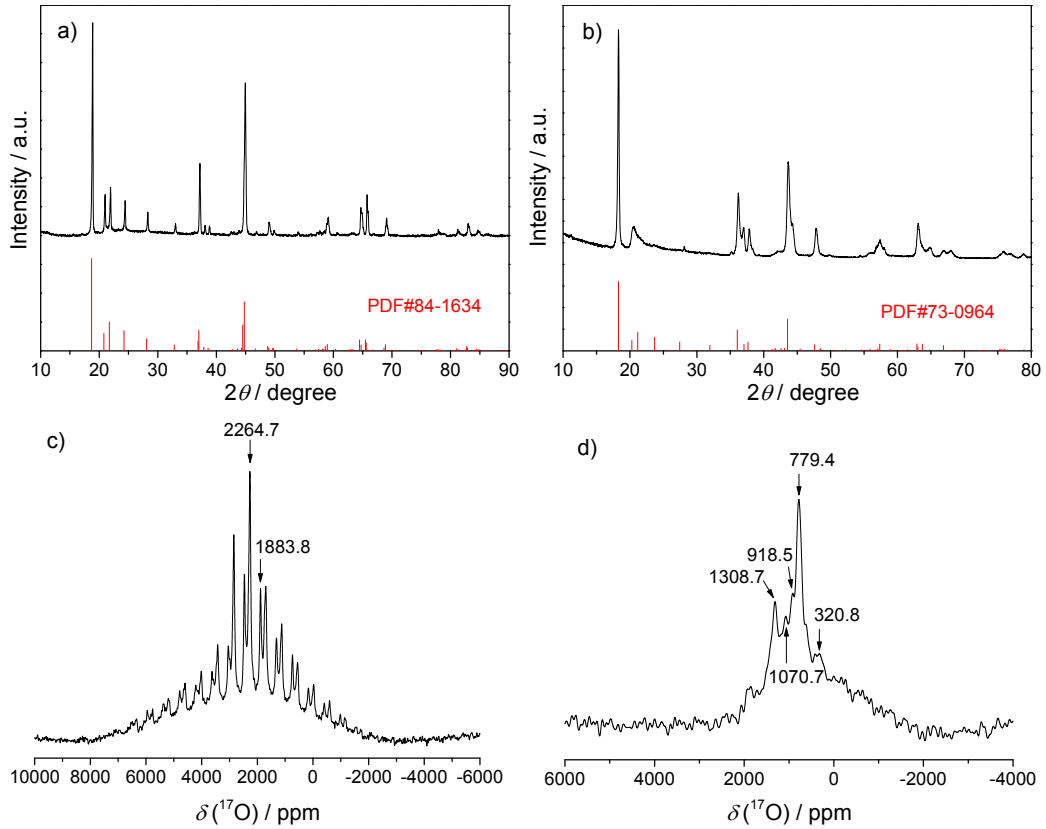

Figure S3. XRD pattern (a, b) and ^{17}O NMR spectrum (c, d) of the ^{17}O-labeled Li_2MnO_3 and the ^{17}O-labeled Li_2RuO_3 respectively. ^{17}O NMR were acquired with a rotor-synchronized Hahn-echo sequence with a $\pi/2$ pulse width of 1.0 μs at a spinning speed of 47 kHz for Li_2MnO_3 and 45 kHz for Li_2RuO_3, with a recycle delay of 0.01 s, by adding 1,122,215 and 3,417,165 transients respectively. The well distinct superlattice peaks at $2\theta = 20 \sim 35°$ in (a) indicate the ordered stacking of the $Li_{1/3}Mn_{2/3}$ layers, while the broad superlattice peaks at $2\theta = 20 \sim 35°$ in (b) indicate the stacking faults of the $Li_{1/3}Ru_{2/3}$ layers because it is easy to form Ru–Ru dimerizations.[6] The isotropic peak positions in (c) are in good agreement with previous study.[7] The signals in (d) are hard to assign due to the complicated environment of Ru–Ru dimers. The results prove our labeling is economical and efficient because both spectra can be recorded with good signal to noise whthin relatively limited time.

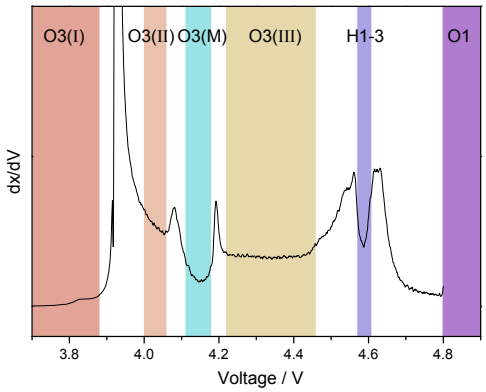

Figure S4. The dx/dV vs. V plot of the $LiCoO_2$ charge curve marked with the corresponding phase regions.

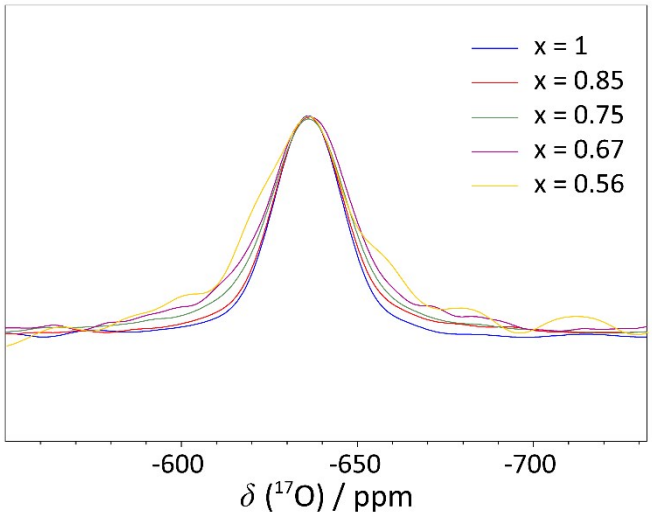

Figure S5. Comparison for the peak width of the isotropic ^{17}O signals at –636 ppm.

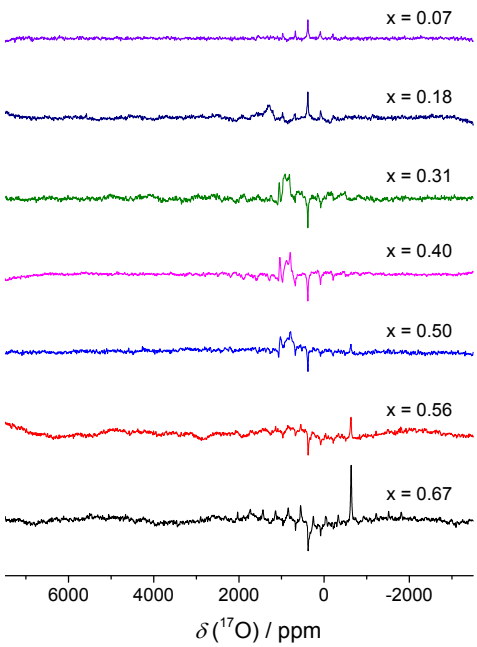

Figure S6. ^{17}O NMR spectra recorded within a wider frequency window for Li_xCoO_2 at x = 0.67, 0.56, 0.50, 0.40, 0.31, 0.18, and 0.07 respectively.

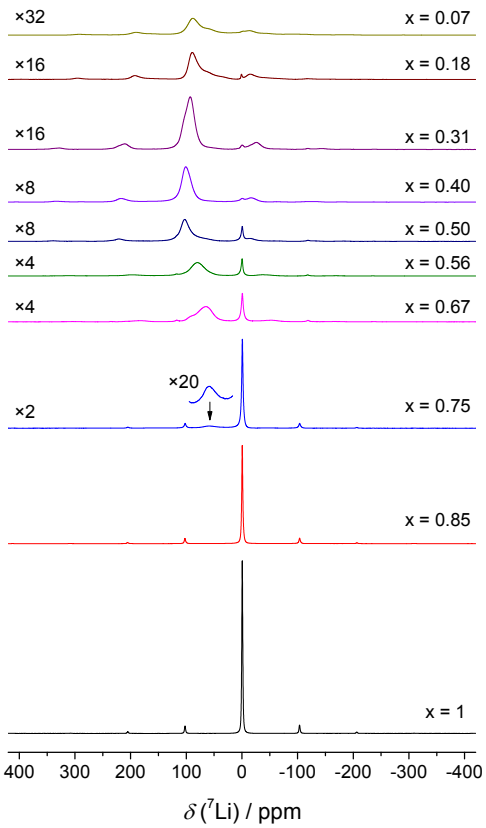

Figure S7. Ex situ ^{7}Li NMR of Li_xCoO_2 at x = 1.0, 0.85, 0.75, 0.67, 0.56, 0.50, 0.40, 0.31, 0.18, and 0.07 respectively.

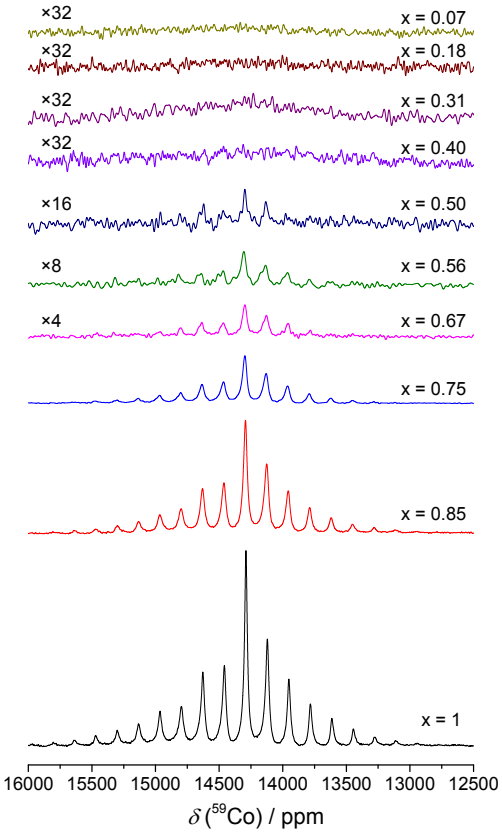

Figure S8. Ex situ ^{59}Co NMR of Li_xCoO_2 at x = 1.0, 0.85, 0.75, 0.67, 0.56, 0.50, 0.40, 0.31, 0.18, and 0.07 respectively.

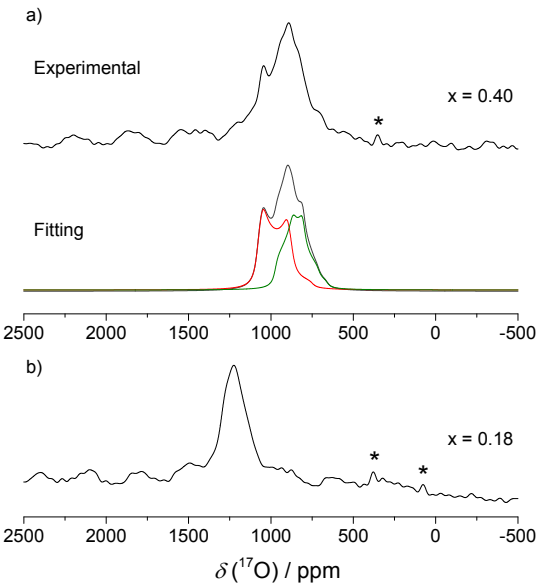

Figure S9. ^{17}O MAS NMR spectra of Li_xCoO_2 at x = 0.4 (a) and x = 0.18 (b) acquired with a rotor-synchronized Hahn-echo sequence. The best second-order quadrupolar fitting (a) results in two oxygen sites with δ_{iso} = 1120, 981 ppm, C_Q = 7.22, 7.98 MHz, η = 0.15, 0.61, and an intensity ratio of 0.97:1 respectively. Asterisks indicate the signal from the zirconia rotor and its spinning sidebands.

References:

S1. R. Siegel, J. Hirschinger, D. Carlier, S. Matar, M. Ménétrier and C. Delmas, *J Phys Chem B*, 2001, **105**, 4166-4174.

S2. M.P.J. Peeters, M.J. van Bommel, P.M.C. Neilen-ten Wolde, H.A.M. van Hal, W.C. Keur, A.P.M. Kentgens, *Solid State Ionics*, 1998, **112**, 41-52.

S3. D. Massiot, F. Fayon, M. Capron, I. King, S. Le Calvé, B. Alonso, J. Durand, B. Bujoli, Z. Gan and G. Hoatson, *Magn Reson Chem*, 2002, **40**, 70-76.

S4. C. P. Grey and N. Dupré, *Chem Rev*, 2004, **104**, 4493-4512.

S5. X. Kong, V. V. Terskikh, R. L. Khade, L. Yang, A. Rorick, Y. Zhang, P. He, Y. Huang and G. Wu, *Angew Chem Int Edit*, 2015, **54**, 4753-4757.

S6. P. J. Reeves, I. D. Seymour, K. J. Griffith and C. P. Grey, *Chem Mater*, 2019. DOI: 10.1021/acs.chemmater.8b05178.

S7. I. D. Seymour, D. S. Middlemiss, D. M. Halat, N. M. Trease, A. J. Pell and C. P. Grey, *J Am Chem Soc*, 2016, **138**, 9405-9408.